Chapter 4

The fate of micropollutants and byproduct formation during the disinfection of WWTP discharge by PFA

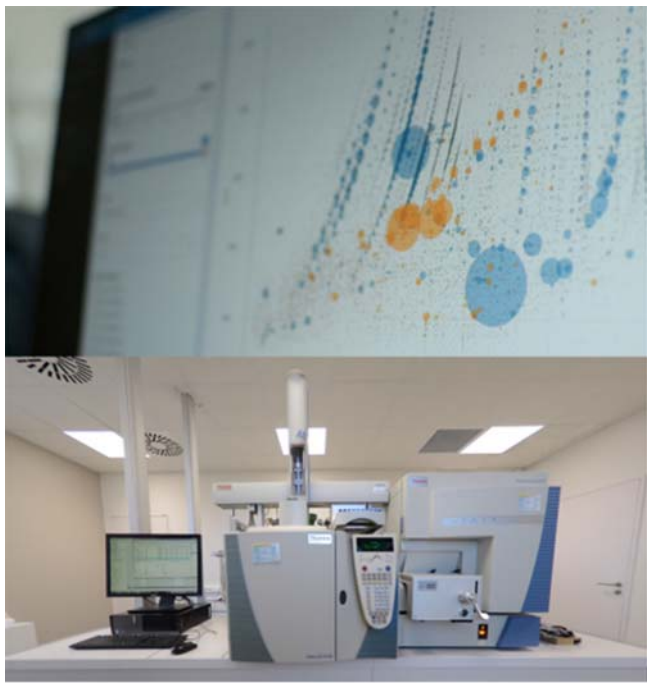

© Julien Le Roux, LEESU

doi: 10.2166/9781789062106_0039

4.1 INTRODUCTION

It is well documented that disinfectants commonly applied during water treatment processes (e.g., free chlorine, monochloramine, chlorine dioxide, ozone) can react with natural organic matter and inorganic ions (e.g., chloride, bromide, iodide) to generate disinfection byproducts (DBPs). The formation of DBPs is undesirable given that the majority of them have been characterized as carcinogenic and mutagenic (Wagner & Plewa, 2017). Since the discovery of chloroform formation from chlorinated organic matter in the 1970s, over 600 DBPs have been identified in disinfected water (Richardson *et al.*, 2007). However, a large proportion of the DBPs generated during disinfection processes remain unknown. It was reported that the identified DBPs only account for less than 50% of total organic halogens during chlorination (Krasner *et al.*, 2006). *In vitro* mammalian cell tests have demonstrated that nitrogenous DBPs (e.g., haloacetonitriles (HANs)) are more cytotoxic and genotoxic than trihalomethanes (THMs) and haloacetic acids (HAAs), which are commonly formed and regulated in drinking water (Plewa *et al.*, 2008). Generally speaking, brominated and iodinated DBPs are also more potent than their chlorinated analogues (Richardson *et al.*, 2007).

N-nitrosamines are a class of emerging nitrogenous DBPs of great concern due to their extremely high carcinogenicity. N-nitrodimethylamine (NDMA), which is the most frequently observed N-nitrosamine, presents a high risk to cause cancer with a probability of one in a million while exposed to a 0.7 ng/L solution (Mitch *et al.*, 2003). Its high polarity enables easy passage through reverse osmosis membranes during wastewater reclamation processes, thus necessitating the use of UV photolysis to remove it from the produced water supply (Mitch *et al.*, 2003). Previous studies have demonstrated that most N-nitrosamines originate from the dissolved organic nitrogen present in wastewater, and especially from secondary and tertiary amines (Schreiber & Mitch, 2007). Tertiary amines in anthropogenic compounds (e.g., pharmaceuticals, pesticides) (Le Roux *et al.*, 2011) and amine-based coagulation polymers (Park *et al.*, 2009) were reported as major precursors of N-nitrosamines. N-nitrosamines are generally present at low ng/L levels in drinking water, hence their detection requires robust analytical techniques (e.g., pre-concentration, tandem mass spectrometry) to reach low detection limits (Alexandrou *et al.*, 2018). Despite their typically low occurrence and concentrations, levels over 1000 ng/L were however reported in wastewater (Bond *et al.*, 2011). The reliance on chloramination as a disinfection process is known as a major source of N-nitrosamine formation. Break point chlorination (especially in the presence of nitrite ions), the ozonation of compounds containing dimethylamine groups and the sunlight treatment of nitrite-containing water are also known to generate N-nitrosamines (Shah & Mitch, 2012).

In recent years, peracids such as peracetic acid (PAA) and performic acid (PFA) have received increasing attention as alternatives to chlorine-based disinfectants (Domínguez Henao *et al.*, 2018). Previous studies have reported that high PAA

concentrations (>30 mg/L) lead to the formation of brominated byproducts, including bromoform, dibromochloromethane and brominated phenols, in bromide ion-enriched solutions (Dell'Erba *et al.*, 2007; Shah *et al.*, 2015). PAA slowly reacts with chloride, bromide and iodide ions in water to generate secondary oxidants (i.e., hypochlorous (HOCl), hypobromous (HOBr) and hypoiodous acids (HOI)) in accordance with Equations (1)–(3) (k values were adapted from (Shah *et al.*, 2015)):

$$CH_3COOOH + Cl^- \rightarrow HOCl + CH_3COO^- \quad k = 1.47 \times 10^{-5}\,M^{-1}s^{-1} \quad (1)$$

$$CH_3COOOH + Br^- \rightarrow HOBr + CH_3COO^- \quad k = 0.24\,M^{-1}s^{-1} \quad (2)$$

$$CH_3COOOH + I^- \rightarrow HOI + CH_3COO^- \quad k = 4.2 \times 10^{2}M^{-1}s^{-1} \quad (3)$$

These secondary oxidants can further react with organic matter to generate halogenated byproducts. HOBr is highly reactive with electron-rich moieties (e.g., activated aromatic rings, amines), with second-order rate constants up to three orders of magnitude higher than HOCl, and moreover forms brominated DBPs (Heeb *et al.*, 2014). However, under commonly applied water treatment conditions (PAA <10 mg/L), PAA produces less DBPs compared to chlorine or ozone (Kitis, 2004).

Furthermore, the residual H_2O_2 in peracid solutions can also play a role as an oxidant; it was reported that under acidic conditions, H_2O_2 also generates HOBr according to Equation (4) (Dell'Erba *et al.*, 2007):

$$H_2O_2 + Br^- + H^+ \rightarrow HOBr + H_2O \quad (4)$$

However, the H_2O_2 residual in water also acts as a sink for secondary oxidants; H_2O_2 reduces the free chlorine and bromine to chloride and bromide, respectively (Equations (5) and (6)) (Held *et al.*, 1978; Shah *et al.*, 2015):

$$H_2O_2 + HOCl \rightarrow Cl^- + {}^1O_2 + H_2O + H^+ \quad (5)$$

$$H_2O_2 + HOBr \rightarrow Br^- + {}^1O_2 + H_2O + H^+ \quad (6)$$

The presence of excess H_2O_2 in water may therefore reduce the formation of DBPs by consuming the secondary oxidants.

Similar to PAA, PFA is a powerful oxidant (Chhetri *et al.*, 2014) that can potentially react with organic matter and inorganic halides present in wastewater effluent. To the best of our knowledge, little is known about the potential formation of DBPs during the disinfection of wastewater effluent with PFA. A previous study reported that no DBPs (e.g., bromoform, detection limit: 0.5 µg/L) were found in wastewater disinfected with PFA (1 mg/L) and containing 0.4 mg/L bromide (Ragazzo *et al.*, 2013). Few studies have evaluated the formation of N-nitrosamines during PAA disinfection processes, but none regarding PFA processes. It was also reported that in the presence of 100 µg/L of amine precursors, 5 mg/L of PAA did not produce N-nitrosamines above the

detection limit within 7 days of contact time, except for the formation of 8 ng/L of N-nitrosodipropylamine (NDPA) (West *et al.*, 2016).

In recent years, non-targeted analytical methods have generated interest in monitoring the evolution of organic compounds in the environment or during water treatment processes, thanks to the evolution of high-resolution mass spectrometry (HRMS). The goal of non-targeted screening is to detect as many ions as possible by means of HRMS in order to obtain an overview of the organic compounds present in a sample as well as to identify specific unknown molecules. Based on the accurate mass of each ion detected in a chromatogram, tentative molecular formulae are assigned and molecular structures can be derived, ultimately by searching in a library and injecting the corresponding analytical standard (if available) (Schymanski *et al.*, 2015). Chromatograms obtained by non-targeted analyses contain many compounds and thus generate large datasets that need to be examined using statistical tools. Such tools are commonly employed in metabolomics studies (Boccard *et al.*, 2010; Ramadan *et al.*, 2006) to: process a large number of variables, determine trends (e.g., increase of a signal over time), or identify molecules of interest in specific samples, for example, by searching for the compounds responsible for differentiating between groups of samples (Poulin & Pohnert, 2018; Schollée *et al.*, 2016). These methods have been used to assess the evolution of organic compounds during wastewater treatment processes (i.e., conventional treatment or advanced treatment, such as ozonation or adsorption onto activated carbon) (Bergé *et al.*, 2018; Merel *et al.*, 2017; Nürenberg *et al.*, 2019).

Suspect screening is another approach lying between targeted and non-targeted analyses. As in targeted analyses, a limited list of compounds is defined for suspect screening, based on various criteria such as the occurrence of compounds in previous studies or transformation mechanisms (Schymanski *et al.*, 2015). In contrast with the targeted analysis however, no reference standards are required for suspect screening, thus making it possible to search for compounds that are not commercially available (Krauss *et al.*, 2010). Consequently, confirmation and quantitation cannot take place during suspect screening, although the information related to the structure and molecular formula does prove to be helpful in proposing the presence of the compounds of interest in a sample analyzed by HRMS.

The primary purpose of this study has been to investigate the formation of DBPs during PFA-based disinfection of wastewater treatment plant (WWTP) discharge at both laboratory and industrial scales. Three classes of known DBPs were targeted: trihalomethanes (THMs), haloacetonitriles (HANs), and N-nitrosamines. Adsorbable Organic Halogens (AOX) were also analyzed in order to determine the formation of total halogenated organic compounds. The second objective of the study has been to characterize the evolution in organic micropollutants both before and after PFA disinfection by means of HRMS analysis. First, a non-targeted screening approach was applied to accomplish the global characterization of each sample, including total number of peaks and their total intensity, as well as

the average retention time and average m/z of each peak. Second, a suspect screening was conducted based on a comprehensive list of 201 anthropogenic organic micropollutants (e.g., pesticides, pharmaceuticals, drugs), which had previously been detected in raw and/or treated wastewater (Bergé *et al.*, 2018; Mailler *et al.*, 2016, 2017).

4.2 TARGETED SCREENING OF DISINFECTION BYPRODUCTS

4.2.1 Experimental description

Wastewater effluent samples were collected between September 2018 and December 2018 from both the Seine Amont Valenton (SEV) WWTP and the Seine Centre (SEC) WWTP. Treated water (TW) at the SEV WWTP, corresponding to the PFA pilot inlet (see Part 2, Chapter 1) was collected on Sept 11, 2018, Sept 18, 2018 and Nov 6, 2018, and then used for laboratory scale disinfection experiments. Pretreated raw water (RW) and settled water (SW) were collected on Dec 11, 2018 from the SEC WWTP (see Part 1, Chapter 1) and used at the laboratory scale as well. Full-scale disinfection trials were performed on-site at the SEV WWTP; the samples were collected both before (SEV-TW) and after disinfection with PFA (i.e. disinfected water, SEV-DW) on Sept 26, 2018, Oct 10, 2018 and Oct 24, 2018. The experimental conditions applicable to each sample are given in Part 2, Chapter 1 for the full-scale disinfection trial samples. For the laboratory scale trials, 1, 2, 30 and 100 ppm of PFA were applied on TW samples, in addition to 1 ppm after injection of 2 mgN/L of nitrite and just 10 ppm of PFA for RW and SW from SEC.

All chemicals introduced were of analytical grade or higher and used as received without any further purification. A standard mix of chlorinated organics and DBPs, including four trihalomethanes (chloroform, dichlorobromomethane, dibromochloromethane and bromoform) plus three haloacetonitriles (dichloroacetonitrile, chlorobromoacetonitrile and dibromoacetonitrile), dichloropropanone and chloropicrin, was purchased from LGC Standards SARL (Molsheim, France) (100 ng/µL of each compound in acetone). Decafluorobiphenyl (99%) was supplied by Sigma-Aldrich Inc. (St. Louis, MO, USA). Ethyl acetate, Methyl tert-butyl ether (MTBE), sodium nitrate (99.99%) and nitric acid (70% v/v) were all supplied by Merck KGaA (Darmstadt, Germany). 2,4,6-trichlorophenol (98%) was purchased from Acros (Thermo-Fisher Scientific Inc., Waltham, WA, USA). The standard HCl solution (0.01 mol/L) used for the AOX-200 titration cell check was provided by Mitsubishi Chemical Analytech (Japan). The activated carbon for AOX measurements was purchased from Envirotech (Germany).

GC-MS grade dichloromethane (DCM) was purchased from Merck KGaA (Darmstadt, Germany). A mixed standard of N-nitrosamines,

including N-nitrosodibutylamine (NDBA), N-nitrosodiethylamine (NDEA), N-nitrosodimethylamine (NDMA), N-nitrosodiphenylamine (NDPhA), N-nitrosodipropylamine (NDPA), N-nitrosomethylethylamine (NMEA), N-nitrosomorpholine (NMOR), N-nitrosopiperidine (NPIP), N-nitrosopyrrolidine (NPYR) (with 2000 µg/mL of each analyte in DCM) and Toluene-d8 (2000 µg/mL in DCM), were all purchased from Agilent Technologies Inc. (Santa Clara, CA, USA). The N-nitrosodimethylamine-d8 (NDMA-d8) and N-nitrosodipropylamine-d14 (NDPA-d14) (1 mg/mL in DCM) were both supplied by Cambridge Isotope Laboratories Inc. (Tewksbury, UK). Coconut charcoal SPE tubes were supplied by Sigma-Aldrich Inc. (Saint-Louis, MO, USA), and the ultrapure water was produced from Milli-Q IQ 7000 Merck KGaA (Darmstadt, Germany)).

4.2.2 Adsorbable organic halogens (AOX) analysis

AOX were analyzed according to the NF-EN-ISO-9562 standardized method. Fifty mg of activated carbon and 5 mL of $NaNO_3$ (0.2 mol/L) were added to 100 mL of wastewater sample, whose pH had been adjusted to pH <2 with nitric acid. After 1 h of constant stirring, the adsorbed activated carbon was filtered by ceramic frits with Activated Carbon Adsorption Unit SA-200 (Mitsubishi Chemical Analytech, Japan), followed by a nitrate-wash of activated carbon (25 mL, 0.01 mol/L of $NaNO_3$). AOX were then converted into hydrogen halides under high-emperature (950°) combustion of activated carbon with an Adsorbable Organic Halogen Analyzer AOX-200 (Mitsubishi Chemical Analytech, Japan). The hydrogen halide gas produced was then dehydrated and introduced into a titration cell. The limit of quantification in the titration cell was 0.7 µg of Cl. The AOX recovery rate of a standard solution (50 µg/L of 2,4,6-trichlorophenol) was found to equal 100.6%.

4.2.3 Halogenated DBP analysis

THMs and HANs were analyzed after liquid–liquid extraction according to EPA method 551. Samples (50–100 mL) were transferred into 120 mL amber glass bottles containing 10 g of NaCl. Fifty µL of decafluorobiphenyl (10 mg/L in acetone) were spiked as a surrogate standard and 3–6 mL of ethyl acetate were added as the organic solvent for most samples. The sampling bottle was vigorously and consistently shaken by hand for 4 min. The water and organic phases were allowed to separate for 2 min. About 2–3 mL of organic extract was transferred into a smaller vial and evaporated under N_2 gas. Lastly, 200 µL of concentrated extract was transferred into a GC-MS vial and stored at 4°C until analysis.

DBP quantification was performed in electronic ionization mode using a gas chromatograph (Trace GC Ultra, Thermo Fisher Scientific Inc., Waltham, WA, USA), coupled with a triple-quadruple mass spectrometer (TSQ Quantum, Thermo Fisher Scientific Inc., Waltham, MA, USA). One µL of extract was injected (inlet temperature: 200°C) in pulsed splitless mode. The compounds

were separated on a Rxi® 5Sil MS (60 m × 250 µm × 0.25 µm) column (Restek, France). The oven program was held at 35°C for 9 min, ramping up to 125°C at 10°C/min, then increased to 220°C at 25°C/min and held there for 2 min. The total run time was 23.8 min. The DBP standard calibration curve was in the range of 50–500 µg/L in solvent, thus corresponding to a limit of quantification of 0.1 µg/L in water samples before extraction. The DBPs were quantified in single-ion monitoring (SIM) mode.

4.2.4 N-nitrosamine analysis

The extraction and detection method of N-nitrosamines was adapted from both US EPA method 521 and a gas chromatography method coupled with tandem mass spectrometry (GC-MS/MS) (Yoon *et al.*, 2012). One hundred µL of NDMA-d8 and NDPA-d14 (500 µg/L in DCM) were spiked as internal standards into 500 mL of a filtered (GF/F, 0.7 µm pore diameter) sample. The N-nitrosamines were extracted using coconut charcoal solid-phase extraction cartridges (6 g, Sigma-Aldrich Inc., Saint-Louis, MO, USA) using a Dionex™ AutoTrace (ThermoFisher Scientific Inc., Waltham, MA, USA) at a rate of 10 mL/min. The cartridges were conditioned with 5 mL of DCM, 5 mL of methanol and 10 mL of ultrapure water. After extraction, the cartridges were dehydrated for 30 min by purging the N_2. Twelve mL of DCM were used to elute the analytes. The eluate was concentrated by evaporation under a stream of N_2 until ~1 mL. Nine hundred µL of the concentrated extract were accurately transferred into GC-MS vials and stored at –20° until analysis. Forty-five µL of injection standard (Toluene-d8, 2 mg/L in DCM) were added into the extract before injection into GC-MS/MS.

The nine N-nitrosamines (i.e. N-nitrosodibutylamine (NDBA), N-nitrosodiethylamine (NDEA), N-nitrosodimethylamine (NDMA), N-nitrosodiphenylamine (NDPhA), N-nitrosodipropylamine (NDPA), N-nitrosomethylethylamine (NMEA), N-nitrosomorpholine (NMOR), N-nitrosopiperidine (NPIP) and N-nitrosopyrrolidine (NPYR), 2000 µg/mL each in DCM), plus the two internal standards (NDMA-d6 and NDPA-d14) and one injection standard (toluene-d8) were all analyzed in electron ionization mode using a gas chromatograph (Trace GC Ultra, Thermo Fisher Scientific, Waltham, MA, USA) coupled with a triple-quadruple mass spectrometer (TSQ Quantum, Thermo Fisher Scientific Inc., Waltham, MA, USA). One µL of extract was injected (inlet temperature: 250°C) in pulsed splitless mode. Chromatographic separation was completed in an Rxi® 5Sil MS (60 m × 250 µm × 0.25 µm) column (Restek, France). The oven program was held at 45°C for 3 min, ramping up to 130°C at 25°C/min, then increased to 230°C at 12°C/min and held there for 1 min. Total run time was 15.7 min. The calibration standards of N-nitrosamines were prepared in the range of 5–100 µg/L. Internal standards NDMA-d6 and NDPA-d14 were added into each standard as 50 µg/L. The toluene-d8 in calibration standards was 100 µg/L. The N-nitrosamines were quantified in

selected reaction monitoring (SRM) mode using argon (6.0) as the collision gas. The detection parameters (collision energy for each compound) were optimized by injecting a 5 mg/L N-nitrosamine standard solution. Table 4 shows the selected analytical parameters for each N-nitrosamine (retention time, parent and product ions, and collision energies). The limits of quantification of N-nitrosamines were in the range of 0.1–6 ng/L.

4.2.5 Impact of PFA on AOX and halogenated DBP formation in WWTP discharge

Table 5 shows the concentrations of AOX and DBPs found in SEV or SEC wastewater before and after PFA disinfection processes, during both laboratory scale experiments and full-scale trials.

During all disinfection experiments (both at the laboratory scale and during full-scale on-site trials), >30 µg/L of AOX were already present in the wastewater effluent samples before any disinfection steps. At the laboratory scale, the disinfection of wastewater effluent samples using PFA concentrations of 2 and 30 ppm ($C \times t = 20$ and 300 ppm.min, respectively) increased the AOX concentrations by 5–10 µg/L. The disinfection of raw and settled wastewater samples (December 2018) with 10 ppm PFA did not produce any significant amounts of AOX. A high concentration of 100 ppm of PFA ($C \times t = 1000$ ppm.min, November 2018) significantly increased the formation of AOX from 45 to 339 µg/L, thereby indicating that halide ions (probably bromide ions) can be incorporated into organic matter upon reaction with high doses of PFA.

Table 6 presents the bromide ion concentration in SEV WWTP wastewater effluent both before and after full-scale disinfection by PFA (August–October 2018). Bromide ions were present in effluent within the range of 100–250 µg/L, and their concentration varied significantly over time. A decrease of about 10–40% in bromide concentration was observed after PFA treatment in the August–September (but not October) samples, which could be attributed to the reactivity of bromide ions with PFA (e.g., to generate HOBr-like PAA, see Equation (2)).

Among the regulated THMs, chloroform was not detected in any sample. Other halogenated DBPs were not detected in WWTP discharge samples either before or after disinfection using low doses of PFA ($C \times t = 10$–30 ppm.min). At higher PFA doses ($C \times t = 74$, 300 and 1000 ppm.min) and in disinfected raw and settled wastewater, dichlorobromomethane (DCBM), dibromochloromethane (DBCM), bromoform (TBM), bromochloroacetonitrile (BCAN) and dibromoacetonitrile (DBAN) were the most frequently detected DBPs. In most samples where DBPs were detected (except for the 1000 ppm.min PFA dose), DBP concentrations were determined to be less than 1 µg/L. The highest concentrations were observed for samples treated with PFA at 1000 ppm.min (e.g., DCBM = 2.4 µg/L, DBCM = 1.4 µg/L, BCAN = 2.0 µg/L, DBAN = 0.6 µg/L), in agreement with the high

AOX concentrations detected in this sample. Chlorinated DBPs were also formed (TCAN = 0.7 µg/L, DCP = 3.4 µg/L, TCNM = 1.8 µg/L), with DCAN reaching the highest concentration of all DBPs (8.25 µg/L). As shown in Equations (1) and (2), the rate constant of chloride with PAA is four orders of magnitude lower than that of bromide. The PFA rate constants with halide ions are not available. However, our results indicate that brominated DBP may be preferentially formed during PFA disinfection via the formation of HOBr as an intermediate, followed by the formation of HOCl and chlorinated DBPs at higher PFA doses, which would require subsequent confirmation. Furthermore, the formation rate constant of HOI during the PAA reaction with halides is roughly three and seven orders of magnitude higher than that of HOBr and HOCl, respectively (Equation (3)). Further investigation is therefore needed regarding the potential formation of HOI and iodinated DBPs, which may be favored during PFA disinfection. The high reactivity observed at 1000 ppm.min is also in accordance with results obtained using 3D fluorescence spectrometry (see Chapter 3), in showing a significant modification of the organic matter matrix. More specifically, a large decrease was observed for protein-like substances, which are known to be major precursors of nitrogenous DBPs such as HANs (Bond *et al.*, 2011).

An injection of 2 mg N/L of nitrite ions with a PFA dose of 10 ppm.min led to the increased formation of two DBPs (BCAN = 0.15 µg/L, DBAN = 0.10 µg/L), which were not detected in the absence of additional nitrite (November 2018), although the concentrations remained very low. A confirmation of the effect of nitrite ions on halogenated DBP formation would require additional experiments at various nitrite and PFA concentrations.

Low concentrations of DBCM, TBM and DBAN (<0.4 µg/L) were detected in both raw and settled water samples. A slight increase in these DBP concentrations was observed after disinfection of the raw water with 100 ppm.min PFA, but concentrations remained less than 0.5 µg/L.

During the on-site industrial disinfection of the WWTP effluent, no DBPs were detected at the lowest PFA doses (Sept 26, 2018 and Oct 10, 2018, $C \times t = 32.1$ and 28.3 ppm.min, respectively), yet brominated DBPs were detected when a higher dose ($C \times t = 74.2$ ppm.min) was employed, in agreement with results obtained from laboratory batch tests at higher doses (i.e. >100 ppm.min). In particular, an increase of ~0.4 µg/L in DBAN concentration was observed. As in batch experiments, AOX concentrations increased by 6–13 µg/L and were not significantly higher at the highest PFA dose ($C \times t = 74.2$ ppm.min) than those at two other doses ($C \times t = 32.1$ and 28.3 ppm.min).

Overall, the low doses of PFA generally employed to disinfect WWTP discharge (i.e., ~20–30 ppm.min) did not form any detectable amounts of halogenated DBPs, and moreover the concentrations observed at higher doses (>70 ppm.min) were always low compared to other oxidation processes and significantly lower than the regulatory thresholds defined for drinking water (total THMs <100 µg/L). In comparison, the chlorination of SEC WWTP discharge (2 ppm during 10 min in

batch, March 2018) formed ~150 µg/L of AOX, while <10 µg/L of AOX were generated from PFA at a similar dose.

4.2.6 Impact of PFA on N-nitrosamine formation in WWTP discharge

The method performance from solid-phase extraction to GC-MS/MS analysis was monitored based on the recovery rate of NDMA-d6, which was spiked into each wastewater effluent sample with a known concentration (100 ng/L) using toluene-d8 as the injection internal standard. The average recovery was 76.5%, which is consistent with recoveries reported in US EPA method 521 (77.2%) for most N-nitrosamines on similar coconut charcoal cartridges.

Table 7 shows the concentrations of N-nitrosamines in WWTP discharge before and after treatment with PFA. Among the nine targeted N-nitrosamines, NMEA, NPYR and NDPhA were not detected in any of the samples. Less than 5 ng/L of NDEA, NDPA, NPIP and NDBA were found in most samples. Nineteen and 17 ng/L of NDEA and 27 and 30 ng/L of NDMA were present in the raw and settled water samples (December 2018), respectively. NDMA was the most abundant nitrosamine detected in the WWTP discharge (treated water) samples (19–33 ng/L, average: 28 ng/L), followed by NMOR (6–18 ng/L, average: 11 ng/L), at levels commonly reported in the literature. NDMA and NMOR were reported to be the most predominant N-nitrosamines in untreated and treated wastewater (Gerrity *et al.*, 2015; Krauss *et al.*, 2009). Industrial products, such as rubber, tires and dyes, are potential sources of NDMA and NMOR. NDMA can also be produced during cooking (Lee & Oh, 2016). Household products (e.g., laundry detergents, dishwashing soaps) contain morpholine (NMOR precursor) as impurities (Glover *et al.*, 2019).

Statistical analysis (t-tests) indicated the lack of any significant differences in N-nitrosamine concentrations after disinfection with PFA at any concentration rate, even at the highest dose employed (1000 ppm.min). However, the addition of 2 mg N/L of nitrite ions during the PFA disinfection ($C \times t = 10$ ppm.min) of treated water significantly increased the NMOR level, from 14 to 162 ng/L (November 2018). Under acidic conditions, the nitrite ion is known to react with secondary amines to generate N-nitrosamines, but this nitrosation mechanism is very slow at neutral pH (Mirvish, 1975). However, studies have demonstrated that some carbonyl compounds (e.g., formaldehyde) can catalyze the nitrosation at higher pH (6.4–11), via the formation of an aldehyde adduct on secondary amines (Keefer & Roller, 1973). PFA also contains a carbonyl group in its structure and thus could catalyze a nitrosation reaction upon the addition of nitrite. As shown in Table 7, a slight increase in all other N-nitrosamines (except NPIP) also occurred after adding nitrite (November 2018), but to a much lesser extent than that of NMOR. This outcome was possibly correlated with the presence of high levels of NMOR precursors (e.g., morpholine) compared to

other N-nitrosamine precursors. The NDMA concentration reached 30 ng/L after adding 2 mg N/L nitrite and 10 ppm.min PFA, as compared to the 21 ng/L observed in samples before and after disinfection with 10 ppm.min PFA.

The N-nitrosamine results obtained during on-site PFA disinfection of the WWTP discharge (Sept 26, 2018, Oct 10, 2018, Oct 24, 2018) were all in good agreement with results obtained at the laboratory scale. The concentrations of all N-nitrosamines were low (<19 ng/L), except for NDMA which reached 31–33 ng/L in both disinfected and non-disinfected effluents. As in the laboratory scale experiments, NMEA, NPYR and NDPhA were never detected. The concentration of certain N-nitrosamines (e.g., NDEA and NDBA) sometimes increased slightly after PFA disinfection, but this was not systematically observed across the three sampling campaigns, especially not during the campaign with the highest PFA dose (74.2 ppm.min). In considering the potential impact of nitrite ions on N-nitrosamine formation, as observed in laboratory scale experiments, it would have been worthwhile to check the nitrite concentrations in the three treated water samples in order to determine a correlation with the observed increases in NDEA and NDBA, but unfortunately the nitrite ion was not measured during these full-scale tests. NMOR did not show any significant increase during full-scale testing, which means that either its precursors were not present in the wastewater effluent or the nitrite concentration was insufficient to cause nitrosation.

Overall, no significant change was noticed for the NDMA concentration after PFA disinfection at any dose. This finding indicates that the WWTP treated water did not contain any significant concentrations of NDMA precursors and/or nitrite ions, and moreover that PFA does not produce significant amounts of NDMA, the most carcinogenic N-nitrosamine, from wastewater effluent.

4.3 NON-TARGETED INVESTIGATION OF MICROPOLLUTANTS DURING PFA DISINFECTION

4.3.1 Experimental description

All samples collected for DBP quantification were also used for non-targeted screening analyses. The samples were filtered using glass fiber filters with a 2.7 and 0.7-µm pore size (Whatman GF/D and GF/F, respectively) within 24 h of collection. One liter of each sample was acidified to pH 6 with sulfuric acid (98%); also, 40 µL of a mixed solution of internal standards (i.e. bisphenol A-d6, 4-n-octylphenol-d17, 4-octylphenol-diethoxylate and propylparaben-d4) were added to each sample. Solid phase extraction (SPE) is currently the most common technique to concentrate molecules, to ensure their improved detection by HRMS (Hogenboom *et al.*, 2009; Müller *et al.*, 2011; Singer *et al.*, 2016). Many studies have applied *universal* cartridges for SPE (e.g., OASIS HLB) in order to retain a large number of molecules (Ibáñez *et al.*, 2008). The combined

use of various cartridges offers an alternative method to capture diverse substances with distinct physicochemical characteristics (Singer *et al.*, 2016). The samples in this study were extracted using an automatic SPE instrument (AutoTrace, Dionex Corporation, Sunnyvale, CA, USA) with cartridges containing a mix of four different phases (Oasis HLB – Water, ENV+ – Biotage, Strata X-AW – Phenomenex and Strata X-CW – Phenomenex). The cartridges were conditioned with 10 mL of methanol, followed by 10 mL of ultrapure water. After sample extraction, the cartridges were dried under a gentle stream of nitrogen for 30 min. The substances were then eluted with 6 mL of a mixture of methanol/ethyl acetate (50:50) and 1.43% ammonia (35%), followed by 3 mL of a mixture of methanol/ethyl acetate (50:50) and 1.7% formic acid. The extract was evaporated under a stream of nitrogen and reconstituted with 1 mL of ultrapure water and methanol (80:20). All extracts were then filtered with PTFE filters (0.2 µm) and transferred into vials for analysis. A sample of ultrapure water ('extraction blank') was extracted under the same conditions as the actual samples.

The samples were analyzed by means of ultra-high performance liquid chromatography (UPLC) coupled with an ion mobility spectrometer and a high-resolution time-of-flight mass spectrometer (IMS-QTOF) (Vion (Waters Corporation, Milford, MA, USA)). The analytes were separated by an ACQUITY UPLC-BEH C18 column (2.1 × 100 mm, 1.7 µm, Water). Ten µL of each sample were injected at a 0.45 mL/min flow rate. The mobile phase was constituted of: (A) ultrapure water +0.1% formic acid, and (B) acetonitrile +0.1% formic acid, while the gradient was 1 min isocratic with 98% A, a 25-min linear decrease to 2% A, 5 min isocratic with 2% A, and a 4-min equilibration time with 98% A. The UPLC column and samples were maintained at 40 and 10°C, respectively.

The ionization was operated by electrospray (ESI) in positive and negative mode with the following parameters: capillary voltage at 0.80 kV (2.50 kV in negative mode), source temperature at 120°C (100°C in negative mode), desolvation temperature at 500°C (250°C in negative mode), cone gas flow rate at 50 L/h, and desolvation gas flow rate at 1000 L/h (600 L/h in negative mode). A data-independent acquisition was performed in $HDMS^E$ mode to obtain low (6 eV) and high (20–56 eV ramp) collision energy spectra to examine both the precursors and fragments. This acquisition was conducted between 50 and 1000 m/z with a 0.2 s scan time.

Each sample was injected in randomized triplicates to limit the intra-sequence variability caused by the instrument's analytical variability. Injection blanks consisting of mobile phase samples were injected along the sequence, along with a pool sample composed of equal volumes of each sample injected during the sequence. This pool sample was used to evaluate the analytical drift during the sequence. The UNIFI software (Water) was used for data acquisition and preprocessing, including 4D peak detection, isotopes and adduct clustering, in addition to the alignment of detected markers across samples. A list of markers

with corresponding exact mass (m/z ratio), retention time, drift time (ion mobility) and intensity in each sample was generated by UNIFI. This list was also exported as a.csv file for further data analysis using the 'R' software (R Core Team, 2019) to produce global statistics or a *bulk characterization* (total number of markers, total intensity, average retention time, average m/z ratio) and visualizations for purposes of sample comparison. The markers that were unique or common to groups of samples were then isolated to produce Euler diagrams using the *limma* (Ritchie *et al.*, 2015) and *venneuler* (*v1.1-0*; Wilkinson, 2011) packages.

4.3.2 Suspect screening

Suspect screening was performed on the same dataset obtained by the non-targeted acquisition on UPLC-IMS-QTOF. A homemade library was created in the UNIFI software, comprising a list of 201 organic micropollutants with their exact mass (m/z ratio) and molecular structure. During the UNIFI processing step, the molecules of the library were searched in all chromatograms, targeted by their exact mass with a tolerance of 5 ppm. False positives were eliminated based on several criteria, namely: the shape of the detected peak, its retention time (based on the expected retention on the BEH-C18 column), and a fragments match (comparison of fragments obtained in high-energy spectra with fragment-generated *in silico* by UNIFI, as well as with fragments found in open access libraries).

4.3.3 Fate of micropollutants: bulk characterization by non-targeted screening

A total of 114,576 and 114,490 markers were obtained from the UNIFI detection algorithm among all 23 samples in positive and negative mode, respectively. The markers detected in all samples were processed to visualize differences between samples by plotting fingerprints based on their retention time, m/z ratio and intensity (Figure 21). This type of plot indicates a systematic decrease in marker intensity after PFA treatment for each type of sample. Modifications to the molecule type were also recorded: many high intensity markers observed at retention times longer than 15 min and with high molecular weights ($>400\ m/z$) disappeared, while other markers detected at shorter retention times (5–12 min) and lower molecular weights (200–400 m/z) exhibited an increase in intensity. This observation was even more pronounced at higher PFA doses (300 and 1000 ppm.min, data not shown), which indicates that PFA can decompose moderately hydrophobic compounds with high molecular weights and, to a lesser extent, produce low molecular weight molecules that are also more hydrophilic. This type of organic compound transformation is typical of other oxidation processes (e.g. chlorination, ozonation). Such information reveals that PFA, in addition to its disinfecting power, is able to both reduce the concentration of many organic compounds and modify to some extent the nature of molecules present in

wastewater effluent. It is worth noting that the WWTP discharge sampled on Sept 18, 2018 (SEV-TW) exhibited a very different fingerprint (not shown), with very large peaks around 8 min, 400 m/z and nearly no difference (i.e. limited decrease in intensity) after a PFA treatment at 20 ppm.min. This outcome was attributed to a degraded water quality due to a bypass of the tertiary phosphorus removal step that occurred in the SEV WWTP during a rain event on Sept 18, 2018 (see Part 2, Chapter 1). Total phosphorus in this sample was 2.5 mgP/L vs. 0.8–1.0 mgP/L under nominal conditions (e.g., SEV-TW from Sept 11, 2018 and Nov 6, 2018). The absence of the coagulation step normally used for phosphorus removal may also degrade water quality through the presence of colloidal matter capable of adversely affecting PFA effectiveness, leading to a degradation of organic compounds. The presence of colloids can also affect the sample preparation step (i.e., SPE), which was reflected in the strong variability observed between replicate fingerprints of this lone sample (i.e., higher variations between marker intensities of the three replicate injections).

A bulk characterization of each sample was performed in order to obtain average information from an entire fingerprint: average retention time, average m/z ratio of the detected markers, plus total number and total intensity (sum of intensities from each individual marker) of all detected markers. This characterization step was first completed with no prior filter (i.e. no threshold on intensities) for each treated water sample before any PFA disinfection (all six SEV-TW samples) and after PFA disinfection at either the full scale (three SEV-DW samples) or the laboratory scale with 20 ppm.min PFA (SEV-TW + 2 ppm PFA). The results obtained for the six samples before and after PFA disinfection were averaged and are summarized in Table 8. The average m/z ratio decreased after PFA treatment, thus supporting the previous observation that organic compounds had a lower molecular weight after oxidation. Retention times and the total number of markers on the whole remained stable, while the total intensity slightly decreased (from 4.8×10^8 to 4.1×10^8), which confirmed the overall reduction in peak intensities visually observed on the fingerprints (Figure 21). These parameters were also calculated from markers detected only before *or* after PFA disinfection (i.e., by removing common markers present both before *and* after PFA treatment). This calculation also clearly confirmed that molecules disappearing after PFA treatment had a higher molecular weight than organic compounds formed after PFA addition, yet the overall slight increase in average retention times did not support the expected formation of more hydrophilic degradation products. The number of molecules appearing after treatment (2,119) was higher than that of the disappeared compounds (1799), but their overall intensity was lower (4.1×10^7 vs. 4.5×10^7).

An intensity value threshold (>10,000) was applied to filter out the smallest peaks that were closer to noise peaks (the intensity values of individual markers ranged between 50 and 41×10^6, and peaks with intensity <10,000 were mainly present in blank samples). Approximately 60% of all markers were still present

after applying this threshold. The total number of markers slightly decreased (from 7369 to 6222, see Table 8) after PFA treatment, as did their total intensity. When considering unique markers, the number of markers formed after PFA treatment (1303) was lower than the number that were totally decomposed (1792), while their overall intensity was slightly lower.

Euler diagrams (Figure 22) allow visualizing the number of markers exclusively present before or after PFA disinfection (i.e., unique markers in Table 8), as well as the number of markers present both before and after treatment (with no indication of their intensity). A clear decrease in the number of markers is observed after treatment (20 ppm.min of PFA) in both positive and negative ionization modes. A small proportion of new peaks was generated during the treatment and can be labeled as decomposition products (i.e. ~18 and ~10% of all peaks present after PFA treatment in positive and negative mode, respectively). A substantial proportion of markers initially present in the WWTP discharge were still present after PFA treatment (i.e. ~34 and ~52% in positive and negative mode, respectively). Similar Euler diagrams were obtained from other samples (data not shown), thus confirming the qualitative observations made from marker fingerprints (Figure 21) that PFA treatment reduces the number of organic compounds detected in the samples.

The overall slight decrease in the average number of markers across all samples after PFA disinfection (Table 8) is detailed for each sample in Figure 23. Some samples (e.g., on Sept 11, 2018 or Nov 6, 2018) exhibited a clear decrease in the number of markers, while all other samples showed no decrease or even a slight increase (especially on Sept 18, 2018, Oct 10, 2018 and Oct 24, 2018). These differences could be attributed to the occurrence of bypasses in the WWTP during the rain events that occurred on Sept 18, 2018, Sept 26, 2018 and Oct 10, 2018, and thus to variations in the WWTP discharge matrix. However, an increase in the number of markers was also observed on Oct 24, 2018 on a date when no bypass occurred, so other unknown factors may have played a role. These results show that the reactivity of PFA with organic molecules can be quite variable depending on underlying conditions (e.g., quality of the wastewater matrix, presence of inorganic ions, temperature). In most cases, the impact of PFA on the number and intensity of markers was very limited. On Nov 6, 2018, the number of markers decreased with an increase in PFA concentration to 1 and 2 ppm, but then increased again at higher PFA doses (30 and 100 ppm of PFA). This finding can be attributed to the formation of additional degradation products, which were indeed observed in the lower range of molecular weight and retention time on fingerprints; it is also in accordance with the higher occurrence of AOX and halogenated DBPs analyzed in these samples. Nonetheless, the number of markers did not exceed that of the initial WWTP discharge. The presence of nitrite ions seemed to decrease the number of markers detected after treatment with 1 ppm PFA, but this assertion would require further confirmation. Lastly, the disinfection of raw (SEC-RW) and settled (SEC-SW)

wastewater (Dec 11, 2018) did not reveal any significant difference in the number of detected markers.

Similar results were obtained by calculating the total intensity of markers in each sample (data not shown), thus demonstrating that the overall concentration of molecules slightly decreased after PFA disinfection and moreover that molecules produced during PFA treatment were not of high intensity. The overall limited decrease in number of markers, as well as the limited formation of organic compounds at low retention times (i.e., more hydrophilic molecules) as described earlier, is in accordance with the low reactivity of PFA in forming DBPs; it is also in agreement with the low impact observed on the organic matter matrix by means of fluorescence spectroscopy measurements (Chapter 3).

4.3.4 Identification and fate of micropollutants characterized by suspect screening

A suspect screening approach was employed on HRMS datasets in order to study the impact of PFA disinfection on specific organic compounds detected in the samples. This suspect screening was performed on a list of 201 anthropogenic organic micropollutants (e.g., pesticides, pharmaceuticals, drugs) that had been previously detected in raw wastewater and/or treated water before discharge (Bergé *et al.*, 2018; Mailler *et al.*, 2016, 2017).

Many of the listed molecules were detected in at least one sample (as revealed by the number of molecules detected in the pool sample). No significant differences were observed between the number of molecules detected before and after PFA disinfection, even at the highest doses (300 and 1000 ppm.min). The intensity of the selected molecules was isolated and corrected by internal standard signals (propylparaben-d4 intensity in each sample) in order to compensate for any deviation between samples. Figure 24 describes the evolution in the pharmaceuticals acetaminophen and sulfamethoxazole, as well as that of 11-nor-9-carboxy-tetrahydrocannabinol, the main metabolite of the psychoactive substance tetrahydrocannabinol (THC) in the samples. These molecules were detected at a high occurrence and relatively high concentrations in raw (e.g., acetaminophen $>100\ \mu g/L$, sulfamethoxazole >500 ng/L) and treated wastewater (Guillossou *et al.*, 2019). These three molecules exhibited a decrease in intensity in most disinfected samples. This result illustrates the moderate degradation of organic micropollutants by PFA and furthermore explains that most molecules were still detected even after PFA treatment.

The individual intensities of each organic compound were averaged by category of molecule, then normalized and reported at increasing PFA doses (0, 10 and 20 ppm.min) from the WWTP discharge sample of Nov 6, 2018 (Figure 25). Once again, most families of molecules exhibited a slight decrease in average intensity at 10 ppm.min and remained stable as the PFA dose was increased to 20 ppm. min. Some categories (e.g. radiocontrast agents, hormones, antibiotics) showed

higher removals, with an average intensity decreasing by more than 50%. Alkylphenols displayed a slight decrease at 10 ppm.min of PFA, but a major increase when 20 ppm.min of PFA were used. This finding could be attributed to the degradation of long-chain alkylphenols and their ethoxylates present in treated wastewater (originating from agricultural, industrial and household products, Bergé *et al.*, 2012), which could react with PFA to produce the simple alkylphenols (e.g., 4-nonylphenol and 4-tert-octylphenol) listed and used in this suspect screening approach. All these results should be carefully considered as qualitative information and would require confirmation by targeted analyses of the organic micropollutants (i.e., a precise quantification by using analytical standards and calibration curves).

Key points

- Disinfection of the WWTP discharge with moderate doses of PFA (10–30 ppm.min) did not generate any detectable amounts of known halogenated DBPs (e.g., THMs, HANs). AOX concentrations generally increased by 5–10 μg/L from the initial 30–40 μg/L concentrations in WWTP discharge. Higher PFA doses (>70 ppm.min) generated low concentrations of halogenated DBPs (DCBM, DBCM, TBM, BCAN and DBAN), which were well below the regulatory threshold for drinking water (e.g. European Union Standards: total THMs = 100 μg/L).
- Low concentrations of N-nitrosamines were detected in the WWTP discharge, with NDMA being the most abundant (up to 33 ng/L). On the whole, no significant change was noticed in the concentration of any N-nitrosamine after PFA disinfection at any dose, which indicates that the WWTP treated water did not contain significant concentrations of N-nitrosamine precursors and/or that PFA is not capable of producing N-nitrosamines. A large increase in NMOR concentration was however detected in the presence of nitrite ions (2 mg N/L) at a low PFA dose (10 ppm.min). This finding should be confirmed by mechanistic studies using NMOR precursors (e.g., morpholine).
- Non-targeted screening by HRMS showed a low reactivity of PFA with organic compounds. Some decomposition of organic molecules was observed even at low PFA doses but was not responsible for producing a substantial number of new molecules (i.e., degradation products), hence in agreement with the low formation of DBPs. Higher PFA doses did increase the number of molecules detected by HRMS, as compared to the low doses by generating degradation products, yet this production never exceeded the number and total intensity of signals observed in the initial WWTP discharge.
- Selected organic micropollutants were just slightly decomposed by commonly employed doses of PFA (10–30 ppm.min). Most categories of

micropollutants exhibited a low reactivity with PFA. Some categories (e.g., radiocontrast agents, alkylphenols) displayed higher reactivity.

- Forthcoming work on HRMS datasets will be dedicated to identifying unknown molecules specific to the wastewater disinfected by PFA, through the use of statistical tools (e.g., principal component analysis, orthogonal partial least squares discriminant analysis) to potentially identify degradation products of interest.
- The overall low reactivity of low doses of PFA towards both the degradation of organic compounds and the formation of DBPs was in agreement with the low reactivity of PFA with the organic matter matrix, as observed by fluorescence spectrometry (Chapter 3).